The Wavelength Dependence of *tert*-Butyl Nitrite Surface Photochemistry

Hans G. Jenniskens, Laurent Philippe,† Malcolm Kadodwala,‡ and Aart W. Kleyn*

FOM-Institute for Atomic and Molecular Physics, Kruislaan 407, 1098 SJ Amsterdam, Netherlands

Received: November 25, 1997; In Final Form: July 27, 1998

The surface photochemistry of *tert*-butyl nitrite adsorbed on Ag(111) was investigated at 532 and 266 nm. The desorbing molecules were detected in time of flight (TOF) mode by a mass spectrometer. Irradiation of the adsorbates leads to desorption of NO at both wavelengths. At these wavelengths caging and bimodal NO TOF distributions, consisting of a hyperthermal and a thermal component, are observed. At 532 nm dissociation is governed by a direct excitation with a cross section of 2×10^{-21} cm^2. The observed TOF distributions at 266 nm are very similar to the 355 nm results, although generally higher translational energies and cross section values (2×10^{-19} cm^2) were measured. At 266 nm dissociation proceeds via a direct excitation. The results are consistent with an excitation into the S_1 state at 355 nm and excitation into the S_2 state at 266 nm.

1. Introduction

Recently we have investigated the surface photochemistry of *tert*-butyl nitrite adsorbed on Ag(111) at 355 nm.[1,2] From our studies we inferred that dissociation proceeds via the same excitation mechanism as in the gas phase. In this article we will report on the photochemistry at other wavelengths (532 and 266 nm) in order to explore the excitation mechanism in more detail.

The coverage and wavelength dependence of surface photochemistry yield important information on the excitation mechanism.[3−6] The coverage dependence was used to study the dissociation mechanism of *tert*-butyl nitrite at 355 nm corresponding to a photon energy of 3.5 eV.[1,2] In this paper we address the wavelength dependence. If dissociation is governed by a direct excitation, i.e., direct photoabsorption by the molecule, a photon resonance may be observed as is shown for $Mo(CO)_6$ adsorbed on Ag(111).[5] A substrate mediated dissociation process, i.e., photoabsorption by the substrate followed by electron transfer to the molecule, will show a monotonically increasing cross section as a function of photon energy and a fairly constant energy distribution of the photoproducts.[6−8] Since we use the harmonics of a Nd:YAG laser to induce photochemistry, the wavelength dependence is only studied at 532 nm (2.3 eV), 355 nm (3.5 eV), and 266 nm (4.7 eV). Although the substrate mediated process seems the most abundant, the relative unimportance of this process has been seen for a number of systems, see e.g. refs 5,9−13.

The gas phase dissociation of alkyl nitrites (RONO) has been investigated in the visible and UV range.[14−30] These studies reveal a weak dependence of the dissociation upon the alkyl-group in the RONO. Between 300 and 400 nm dissociation into NO and an alkoxy proceeds via the predissociative S_1 state, which has a life time of 125 fs.[26] At wavelengths shorter than 300 nm, dissociation via a dissociative S_2 state results in the same dissociation products.[19,22] The cross sections for dissociation via the S_2 state are typically one order of magnitude larger than for dissociation via the S_1 state.[31] The dissociation energy of TBN is about 1.8 eV; the translational energy content of the NO photoproduct is larger for dissociation via the S_2 state compared to dissociation via the predissociative S_1 state (1.0 eV compared to 0.5 eV).[16,28] The photoabsorption spectrum in the 300−400 nm region shows a vibrational progression ascribed to the N═O stretch in the alkyl nitrite.[26] At wavelengths longer than 400 nm most papers report that no dissociation is present. This conclusion is based upon the sharp decrease in optical absorption of the gas phase molecule going from the S_1 excitation region to longer wavelengths. However, no systematic study on the upper limit of a possible dissociation cross section in the visible region has been performed. Schwartz−Lavi and co-workers do report a preliminary observation of dissociation of *tert*-butyl nitrite down to 500 nm.[32]

tert-Butyl nitrite adsorbs without appreciable dissociation on Ag(111) and forms a monolayer and multilayer structure for temperatures lower than 110 K.[33] The monolayer desorbs at 160 K and the multilayer at 120 K. The sticking coefficient is coverage independent. A coverage scale in terms of monolayers adsorbed could be extracted from the observed saturation of the monolayer TDS peak. This saturation occurred for an exposure of 8×10^{-6} mbars. Upon irradiation with 355 nm photons, the adsorbed *tert*-butyl nitrite photodissociates and desorbing NO molecules are observed.[1,2] In TOF measurements two NO desorption distributions are observed. Cross section measurements reveal that both distributions are formed by the same dissociation process. The slow NO distribution consists of molecules that were thermalized by the silver substrate. This thermalization of NO photoproducts by the substrate is only possible if the NO molecule is produced in either the first or second adsorbed layer. Therefore, the thermal component was found to saturate at a coverage of 2 ML. The hyperthermal component also saturated, but this occurred at a coverage of 5 ML. At coverages higher than five layers hyperthermal NO was measured to the same extend as at a coverage of five layers. This shows that for large coverages the outermost layers are still able to photodissociate but that deeper layers are incapable in producing NO due to caging by the surrounding molecules.[2] A *trans* to *cis* conversion of the *tert*-butyl nitrite, also due to caging, was observed in reflection absorption infrared spectroscopy (RAIRS). In the first adsorbed layer at the surface

† Present address: Laboratoire Dynamique des Ions Atomes et des Molcules, 4 place Jussieu 75250 Paris Cedex 05, France.

‡ Present address: Department of Chemistry, University of Glasgow, Glasgow G12 8QQ, Scotland, UK.

10.1021/jp980325q CCC: $15.00
Published on Web 10/13/1998

caging does not prevent dissociation as was apparent by the presence of thermal NO for large coverages. Direct excitation of the molecule is responsible for dissociation in the multilayer regime. In the monolayer the cross section is the same as in the multilayer, and therefore dissociation is believed to proceed via the same direct excitation mechanism. Photodissociation of *tert*-butyl nitrite on MgF_2 has been studied at 351 nm with both rotational and translational resolution of the NO photoproduct.[34,35] Although these experiments suggest that two desorption channels were active, this could not be seen clearly in the TOF measurements. The wavelength dependence of methyl nitrite, CH_3ONO, at Ag(111) has been studied by Pressley and co-workers in the 400−254 nm range.[10] These authors found that photodissociation was mainly a direct process, and roughly the same wavelength dependence of the cross section was found as for gas phase dissociation. Bimodal velocity distributions with a thermal and hyperthermal component were observed. The thermal component was more pronounced for longer wavelengths.

2. Experimental Section

The experiments are performed in an ultrahigh vacuum (UHV) system with the following analytical tools: thermal desorption spectroscopy (TDS), low energy electron diffraction (LEED), X-ray photoelectron spectroscopy (XPS), Auger electron spectroscopy, reflection absorption infrared spectroscopy (RAIRS), and quadrupole mass spectrometry with time of flight (TOF) detection. The system has a base pressure of 2×10^{-10} mbar and is described in more detail elsewhere.[36,37]

The Ag(111) crystal was polished to give a misalignment of less than 0.1° and has a diameter of 10 mm. The crystal can be cooled to 85 K by using liquid nitrogen and heated to 1000 K by electron bombardment. The electrons have an energy of 400 eV and originate from a hot filament behind the crystal. The temperature is measured by a chromel alumel thermocouple inserted in a hole in the side of the crystal. The crystal is cleaned by cycles of sputtering with 800 eV argon ions at 650 K and annealing at 800 K. Crystal cleanliness was checked by XPS and LEED. All irradiation was done at a surface temperature of 85 K.

The *tert*-butyl nitrite, $(CH_3)_3CONO$, was supplied by Aldrich with a specified purity of 96%. The nitrite was stored in a stainless steel container and freeze−pump−thawed several times before introduction into the vacuum system. The crystal was exposed at 85 K to *tert*-butyl nitrite by backfilling the chamber for typically a few minutes. From the mass spectrometer signal during dosing, an accurate exposure is calculated by a method described elsewhere.[37] After dosing the crystal, the base pressure was allowed to return to its normal value.

A picosecond Nd:YAG laser from Quantel was used to irradiate the sample. The laser produced pulses with a wavelength of 1064 nm at a repetition rate of 10 Hz. The pulses had a maximum energy of 55 mJ and a temporal width of 30 ps (full width at half maximum, FWHM). Using a BBO crystal the fundamental (1064 nm, 1.17 eV) was doubled to give 2.3 eV photons (532 nm). Subsequent doubling in a KDP crystal yielded 4.7 eV photons (266 nm). Before the laser beam entered the vacuum system, a 4 mm pinhole was used to transmit the central part of the beam in order to get a uniform beam profile. For the experiments at 532 nm 5 mJ pulses were used and at 266 nm 0.8 mJ. Due to the positioning of the UV grade fused quartz viewports and the quadrupole mass spectrometer (QMS), light was incident on the crystal at an angle of 52.5° with the surface normal and was reflected out of the vacuum system through another viewport. The molecules detected by the QMS leave the surface with an angle of 7.5° from the normal. Light impinging on the surface was composed of equal amounts of *S* and *P* polarized light. We estimate that the polarization vector makes an angle of about 45° with the surface normal.

The QMS was a Balzers 420 quadrupole mass spectrometer with a 90° off axis channeltron and a crossed beam ionizer. The channeltron was connected to a fast current amplifier that fed the pulses to a multichannel scaler (EG&G, turbo MCS). The spectra were recorded with a 15 μs resolution. The flight distance of the molecules from the surface to the ionizer of the QMS was 13.5 cm. After dosing, six TOF spectra were recorded in succession for respectively 400, 400, 400, 800, 1600, and 3200 laser shots. In this way the exponentially decaying yield can be monitored and the cross section for photodissociation leading to gas phase NO can be extracted. No significant changes were observed in the individual TOF spectra. By summing all the six spectra an accurate determination of the peak positions and peak areas is possible.

The TOF spectra are described by Maxwell−Boltzmann velocity distributions. The fit procedure will be described below, but for a more complete description see ref 2. The equation used to fit the spectra is given by eq 1 and consists of a sum over *N* Maxwell−Boltzmann distributions, an offset, and a time dependent background term.

$$s(t_{\mathrm{MCS}}) = y_0 + \sum_{i=1}^{N}\left(\frac{c_i}{t_{\mathrm{MCS}} - t_0}\right)^4 \exp\left(-\left(\frac{t_i}{t_{\mathrm{MCS}} - t_0}\right)^2\right) + \mathrm{BG}(t_{\mathrm{MCS}} - t_0) \quad (1)$$

In this equation t_{MCS} is the time between the laser shot and the detection of a pulse by the MCS. Parameter y_0 is the offset of the set of spectra due to residual gas in the chamber. Parameter c_i is a normalization parameter for spectrum i, and t_i characterizes the position of peak i. Time t_0 is the time between ionization of the molecule in the QMS and detection by the MCS. This is to correct t_{MCS} to yield the true time of flight from the crystal to the ionizer of the QMS. For NO t_0 was calculated to be 17 μs and kept constant in the fitting procedure. The time dependent background term BG describes the pump tail caused by molecules that are trapped on the walls of the ionizer and other parts of the system. This background term was introduced because the TOF signal only returned to the normal background level after a few milliseconds, whereas all the peaks occurred in the first half ms. For more detail on this topic see refs 1 and 2.

The flux-weighted mean translational energy $\langle E_{\mathrm{trans}} \rangle$ and the characteristic translational temperature $\langle E_{\mathrm{trans}}/2k \rangle$ can be calculated from the parameter t_i by eq 2.

$$\frac{\langle E_{\mathrm{trans}} \rangle}{2k} = \frac{ml^2}{2kt_i^2} \quad (2)$$

In this equation k is Boltzmann's constant, m the mass of the desorbing molecule, and l the distance from the crystal to the ionizer of the QMS.

From the parameters c_i and t_i the yield, Y, which is proportional to the total amount of molecules desorbing into the direction of the mass spectrometer (eq 3), can be extracted. This yield takes the velocity dependent detection probability of the QMS into account and only depends on the experimental geometry used. Since the experimental geometry is not changed in the experiment, Y is a very suitable measure for the yield of

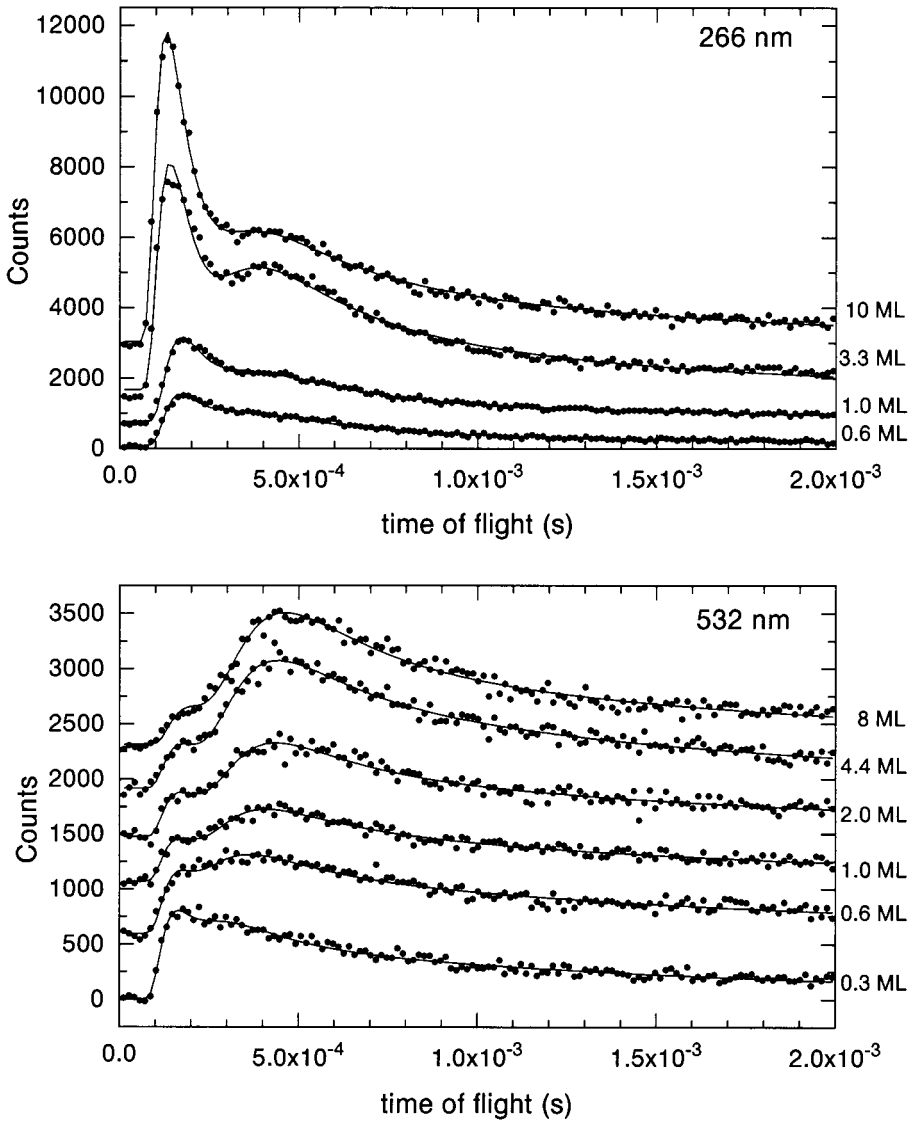

Figure 1. TOF spectra of desorbing NO due to photodissociation of *tert*-butyl nitrite adsorbed on Ag(111) for various coverages. Irradiation was done at a surface temperature of 85 K. The upper panel shows the results for dissociation at 266 nm, and the lower panel shows the results for 532 nm. For both wavelengths bimodal distributions are observed, but the trends are very different.

molecules desorbing into the direction of the QMS. Note that this yield is not angle integrated. When a superposition of two Maxwell−Boltzmann velocity distributions is found, the angular distribution for each channel can be different. Consequently, one cannot obtain the absolute ratio of the total yields for both channels from the ratio of the yields observed at the angle used.

$$Y = \left(\frac{c_i}{t_i}\right)^4 \tag{3}$$

The cross section for photodissociation leading to gas phase NO can be determined by calculating the yield of each of the six TOF spectra obtained from one dose by using eq 3. The cross section determination is based on the principle that the desorption rate of the molecule observed in TOF decays as a single exponential decay as a function of photon dose. By plotting the integrated yield versus the accumulated photon dose in cm^{-2} the cross section can by extracted by curve fitting as described in ref 2. The Gaussian laser beam profile over the crystal has an intensity at the edges of more than 50%. We determined that the resulting error in the determination of the cross section is on the order of 20%, an insignificant amount in view of the very large variations of the cross sections.

3. Results

At a wavelength of 532 nm gas phase dissociation is generally said to be absent. However, we measured a signal for mass 30 in TOF spectra at 532 nm. By performing TOF measurements at other masses we concluded that NO was the only desorbing species. Variation of the laser intensity did not affect the TOF spectrum and the yield appeared to be linear with intensity. Also at 532 nm the TOF spectra are bimodal and consist of a thermal and hyperthermal component. The spectra have been integrated over 6800 shots to build up statistics. However, TOF spectra for a limited number of shots show that there is no dependence of the TOF spectra upon irradiation time for the spectra shown. Obviously, in the case of complete dissociation of a (sub-)monolayer the desorption signal ultimately vanishes. TOF spectra due to 532 nm photons for a variety of coverages ranging from 0.3 to 8 ML are plotted in the lower panel of Figure 1. For all coverages two velocity components are present. The peak position of the fast component remains more or less constant with coverage, whereas the position of the slow component seems to shift to longer times with increasing dose. However, the apparent shift of the slow component is partially due to the superposition of a fast and slow peak with changing

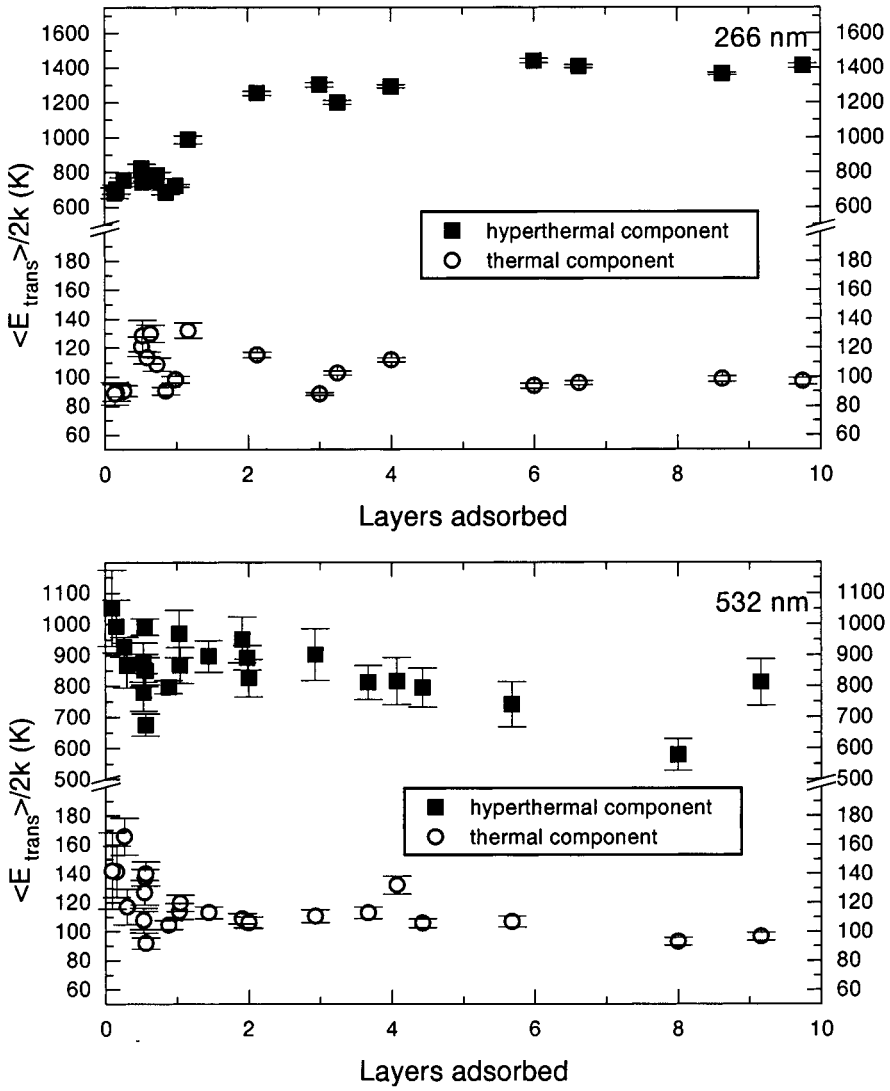

Figure 2. Mean translational energy expressed in K of the desorbing NO distributions as a function of coverage due to 532 and 266 nm irradiation from a 85 K silver substrate. At 532 nm a slight decrease in energy can be observed in the monolayer regime, but at higher coverages no dependence is present. At 266 nm the slow component shows no dependence with coverages. The fast component has a constant energy in the monolayer of about 750 K that increases to 1450 K for a coverage of 5 ML.

relative areas. The relative ratios of the two components show a clear change with coverage. For a coverage of 0.3 ML there is more fast than slow, whereas this ratio is the opposite for higher coverages. For coverages of 2 ML and higher the spectra do not seem to change much, although a slight increase in the amount of slow NO might be present.

At 266 nm (the fourth harmonic of the laser) TOF measurements were also performed. TOF spectra, integrated over 6800 laser shots, are plotted in the upper panel of Figure 1 for several coverages. The spectra and trends are very similar to the 355 nm results.[1] Two components are present in the TOF spectra for all coverages. For high coverages the fast peak dominates over the slow. In the monolayer regime the ratio between the fast and slow component does not change; only for coverages higher than 1 ML does the fast peak increase more than the slow. The spectra do not seem to change for coverages higher than 4 ML, either in yield or in peak positions.

The TOF spectra for 532 and 266 nm are both bimodal for all coverages and the peak positions of the distributions are similar. However, the relative ratios between the two components and the trend with coverage are completely different. Whereas for submonolayer coverages the spectra do resemble each other, for increasing coverage they show opposite trends. For high coverages, at 266 nm the fast component dominates, while at 532 nm the slow component dominates.

To deduce any trends with coverage it is better to decompose the two components by fitting. Because of the overlap of the two components and due to the velocity dependent detection probability of the mass spectrometer, trends could be misinterpreted. Fitting all TOF spectra after 6800 laser shots for different coverages with eq 1 yielded the parameters c_i and t_i. From these parameters the average translational energy $\langle E_{trans}/2k\rangle$ and the yield Y are deduced by using eqs 2 and 3. The uncertainties in the yield and in the translational energy are derived from the standard errors of the fit parameters c_i and t_i.

The average translational energy expressed in K for coverages up to 10 ML are plotted in Figure 2 for both the fast and slow component. In the upper panel the 266 nm results are shown and in the lower panel the 532 nm results. The slow component at 532 nm shows a slight decrease in the monolayer regime from 150 to 100 K. For larger coverages the energy remains about 100 K. This energy is comparable to the substrate temperature of 85 K, and, therefore, similar to the 355 nm, we assume that at 532 nm some of the NO photoproducts get thermalized. The fast component shows a slight decrease in average translational energy in the monolayer regime as well.

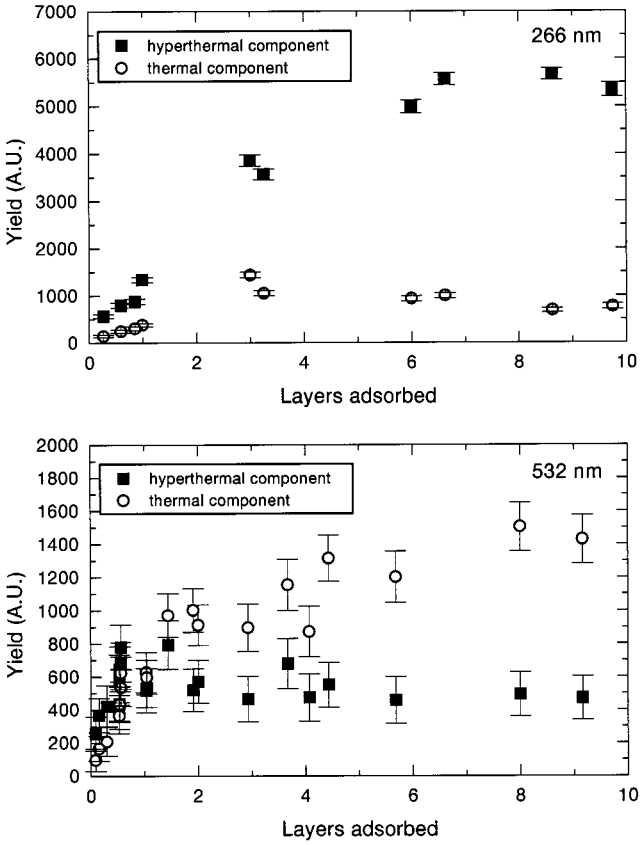

Figure 3. Desorption yield of NO at 532 and 266 nm as a function of coverage for both components. The behavior at 266 nm is very similar to the 355 nm results. At 532 nm the fast component saturates at 1 ML. The slow component increase only slightly above 1 ML and saturates around 5 ML.

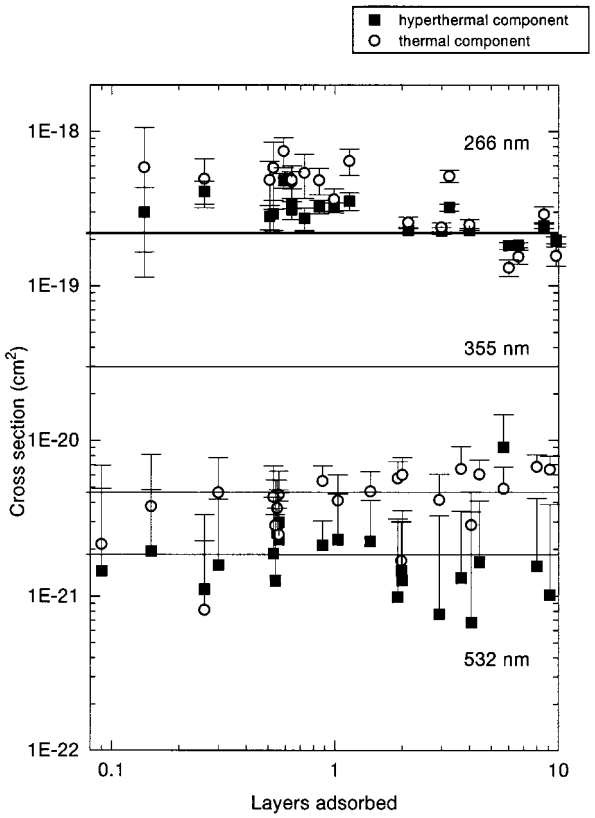

Figure 4. Cross sections for both the thermal and hyperthermal component at 532 and 266 nm. At 532 nm the cross section is independent of coverage. Although the cross section for the thermal component appears to be higher than the hyperthermal cross section, this difference is not significant. At 266 nm the cross sections at low coverage have the tendency to be higher, but since the difference compared to the experimental uncertainty is small, a coverage independent cross section is assumed. For comparison the coverage independent cross section at 355 nm is show (3×10^{-20} cm^2). For clarity, at 532 nm only the upper part of the error bars are shown.

Generally the energy is about 800−900 K and shows no significant change with coverage.

For the slow component at 266 nm a translational temperature is measured that matches the substrate temperature. So, similar to the results at 532 and 355 nm, efficient thermalization process also exists at this wavelength. If, similar to the 355 nm results, the cross sections for the slow and fast distribution are the same, a single dissociation mechanism is present. That this is the case will be shown below. The hyperthermal component has a constant energy of about 750 K in the monolayer regime. Between 1 and 5 ML the energy increases to 1450 K, and above 5 ML the energy is constant again. This behavior is also observed at 355 nm, although in that case the energy in the monolayer was 600 K, and above 5 ML it was 1000 K. An intriguing observation is that although the excess energy (photon energy minus dissociation energy) of the photons at 532 and 266 nm differ by a factor 6 (0.5 and 2.9) the translational energies are very comparable in the monolayer regime.

The yield at 532 nm between a coverage of 0 and 1 ML shows a linear increase with coverage for both components (lower panel of Figure 3). Within the monolayer region the yields of the thermal and hyperthermal component are comparable. At a coverage of 1 ML the hyperthermal component saturates, and the thermal component increases only slightly. At a coverage of 5 ML the thermal component also appears to have saturated; however, the large uncertainty in the data precludes a firmer conclusion. The slight increase of the slow component above 1 ML coverage could originate from a conversion of fast NO to slow NO. But certainly, the rate of increase in yield observed in the monolayer region does not persist beyond 1 ML coverage.

The yield at 266 nm of both components is plotted in the upper panel of Figure 3. Just as with the behavior of the translational energy, the behavior of the yield is very similar to the 355 nm results. The thermal component saturates around 2 ML, and the hyperthermal component saturates at approximately 5 ML.

Using the procedure described in the Experimental Section, the cross section for photodissociation leading to gas phase NO for both velocity components was measured as a function of coverage (Figure 4). The cross section is determined by modeling the decaying desorption rate with a single exponential decay. Therefore this photodissociation cross section is actually an average over all *tert*-butyl nitrite molecules leading to NO desorption. This means that molecules that are not photoactive, for instance due to caging, do not influence this average cross section. The cross section at 532 nm shows no noticeable change with coverage for both components. The average cross sections measured are 5×10^{-21} cm^2 for the thermal component and 2×10^{-21} cm^2 for the hyperthermal component. However, this difference in cross section is not significant as becomes apparent if the ratio of the thermal and hyperthermal cross section is calculated. This ratio measures 2.5 ± 0.5 (value $\pm$ standard deviation). Therefore, similar to the 355 nm results, we conclude that the cross sections for the thermal and hyperthermal component are indistinguishable. This results in an average value of about 3×10^{-21} cm^2 (for comparison: at 355 nm a cross section of 3×10^{-20} cm^2 was found). The

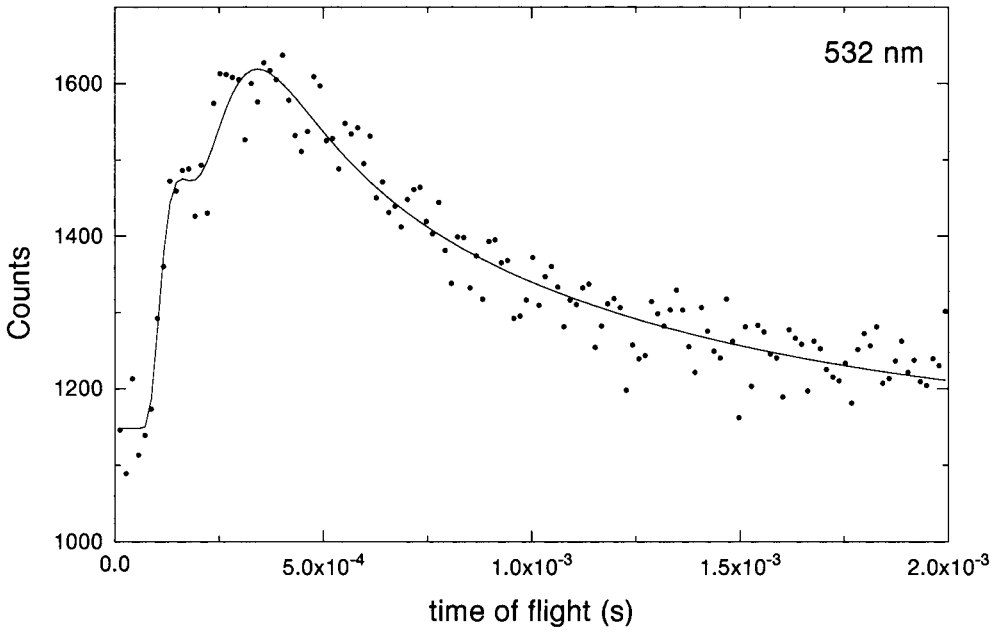

Figure 5. TOF spectrum of 1 ML of *tert*-butyl nitrite on a 20 ML thick methanol spacer layer upon irradiation with 532 nm. The presence of a TOF signal shows that the silver substrate does not participate in the dissociation mechanism. The TOF trace resembles the spectrum obtained from 1 ML of *tert*-butyl nitrite without spacer layer.

error bars in the plot are somewhat larger than those at 355 nm, because the small value of the cross section induces a larger uncertainty.

The cross sections for both the thermal and hyperthermal component at 266 nm are in the 10^{-19} range. For submonolayer coverages the cross sections have the tendency to be slightly higher than in the multilayer regime, but the standard deviations are also larger. If, analogous to previous results, a coverage independent cross section is assumed, a value of 2×10^{-19} cm^2 is obtained. This value is an order of magnitude larger than the cross section at 355 nm. The ratio between the cross sections for the hyperthermal and thermal component is 1.04 $\pm$ 0.04. This strongly suggests that the slow and fast component are produced by the same dissociation process.

The photochemistry at 532 nm has different characteristics than the photochemistry at 355 and 266 nm; therefore, a spacer layer experiment was conducted using methanol. Methanol adsorbed on Ag(111) undergoes no photochemistry up to wavelengths far into the UV.[38] Methanol multilayers desorb at 145 K.[37] These two features allow methanol to be used as a spacer layer molecule. Another characteristic of methanol multilayers is that there are two phases, an amorphous and a crystalline phase.[37] Adsorption of methanol at temperatures lower than 100−110 K results in an amorphous overlayer. Annealing of this layer for 2 min at 120 K causes the conversion into a crystalline phase. The crystalline phase of methanol has been used in the spacer layer experiments, because we expect the diffusion of *tert*-butyl nitrite into the spacer layer to be less for this phase, due to the smaller amounts of defects and cracks.

We have performed spacer layer experiments with 10, 20, and 50 ML of crystalline methanol and 1 ML of *tert*-butyl nitrite adsorbed on top. For all spacer layer thicknesses identical TOF curves were measured. The result for a 20 ML thick methanol spacer layer is shown in Figure 5. The TOF curves obtained from the spacer layer experiment resemble the TOF traces without spacer layer (Figure 1) both in yield, peak position, and ratio of the two components. A detailed analysis shows that the spacer layer experiment systematically results in 20% less NO relative to the 1 ML experiment without spacer layer. Also the slow component of the spacer layer experiment is somewhat faster. These two small differences result in the spacer layer experiment matching better with a 0.8 ML coverage without spacer layer. Thus, although one monolayer is adsorbed, effectively 20% less seems to be photoactive.

4. Discussion

4.1. Photochemistry at 266 nm. The cross section of the slow and fast component at 266 nm are indistinguishable; therefore, we believe that the two components are formed by the same dissociation mechanism. After dissociation of the *tert*-butyl nitrite some NO molecules leave the surface with hyperthermal speed and some NO molecules are thermalized before they can desorb and leave the surface with thermal speed. That the slow component consists of thermalized molecules has been shown for dissociation with 355 nm photons:[1] at this wavelength a correlation between the substrate temperature and the translational temperature of the slow component was measured. The absence of complete translational equilibration for the low rotational NO molecules from MgF_2[34,35] suggests that the metal is needed for complete thermalization. The stronger interaction of NO molecules with the metal compared to MgF_2 observed in adsorption studies is believed to be the cause of this effect.

The yield of both components at 266 nm exhibits the same features as the yield at 355 nm:[2] the thermal component saturates at 1−2 ML and the hyperthermal component saturates at approximately 5 ML. For 266 nm at high coverage the hyperthermal component dominates the thermal component similar to the 355 nm results. Because of all these similarities we conclude that the observed saturation at 266 nm has the same reason as at 355 nm.[1,2] The saturation of the thermal component remains surprising and counterintuitive. Apparently, dissociation within a thick film does not result in separation of the photofragments and diffusion of the NO molecules to the surface of the film where the molecules would thermally desorb. Instead recombination always occurs due to caging. Only when dissociation occurs near the film−substrate interface can the resulting T-butoxy radials form a strong bond to the Ag−

substrate, blocking recombination. Thus, the thermal component saturates because only a dissociation event occurring near the substrate can lead to subsequent trapping of the T-butoxy and thermalization of the NO by the substrate. Dissociation in the third layer and higher will not lead to subsequent thermalization by the substrate, and therefore saturation of the thermal component at 1−2 ML is measured. The saturation of the hyperthermal component at 5 ML is caused by caging in the *tert*-butyl nitrite film. For coverages larger than 5 ML the inner multilayers are caged by the surrounding molecules and therefore do not dissociate. The outermost layers are not caged strongly enough and hence lead to photodissociation products as is apparent by the observation of hyperthermal NO for large coverages. This suggests that hyperthermal NO is able to scatter through several layers without complete thermalization of its translational energy. For ions with a translational energy of a few electronvolts it is shown by the group of Madey that transmission through several layers of rare gasses or water is possible without significant loss of translational energy.[39−41] However, scattering cross sections for fast ions are fairly small, dominated by short range repulsive collisions. In view of the vast body of gas phase rotational relaxation data, suggesting a long range interaction, it is likely that the molecule loses rotational energy quickly when making collisions in the film. This would suggest that for some molecules close to the film surface, there exist "channels" through which the NO can escape without collisions. Another way to achieve the same result would be to assume an extremely rough film, exposing NO in many layers to the outside. Concluding, it seems reasonable to assume that NO photoproducts from a few layers deep can contribute to the hyperthermal component. This proposed mechanism supports dissociation by a direct excitation, because no substrate-mediated mechanism is able to dissociate molecules far away from the substrate. At 355 nm isomerization of the *tert*-butyl nitrite was observed by RAIRS.[2] This was due to photodissociation in the film followed by reassociation in the other isomeric form. This illustrates that both photodissociation leading to a distinct separation of the fragments and caging occurs. We believe that isomerization will also be present at 266 nm. For 355 nm efficient conversion of all *tert*-butyl nitrite was observed in RAIRS up to the point where saturation of the fast component occurred (5 ML). Efficient conversion is expected to be present at 266 nm for coverage up to 5 ML, but the RAIRS has not been carried out.

Above we have mentioned many similarities between the 355 and 266 nm results, but there are also differences. The translational energies at 266 nm are substantially higher. In the monolayer at 266 nm a translational temperature of 750 K was measured compared to 600 K at 355 nm. The multilayer results differ even more: 1450 K for 266 nm compared to 1000 K for 355 nm. This increase by 45% in translational energy in the multilayer going from 355 nm to 266 nm is lower then expected from gas phase experiments where an increase of 100% is measured (2900 K (0.5 eV) at 355 nm to 5800 K (1.0 eV) at 266 nm).[16,28] Another difference is the magnitude of the cross sections. The cross section at 266 nm is an order of magnitude higher. This difference combined with the difference in translational energy at 355 and 266 nm indicates that at these two wavelengths excitation into different excited states occurs, as is found in the gas phase.[26] Dissociation at 355 nm in the gas phase and at the surface was believed to proceed via the S_1 state.[2,26] At 266 nm the present data is consistent with excitation into the dissociative S_2 state. This is also supported by the amount by which the cross section increases going from 355 to 266 nm. In this study we measured an increase by a factor 7 going from 355 to 266 nm (increase from 3×10^{-20} to 2×10^{-19} cm^2). In the gas phase an increase of the same magnitude is measured (from 6×10^{-20} to 5×10^{-19} cm^2).[31] This implies that if dissociation on silver at 266 nm proceeds via the S_2 state, the electronically excited state is not quenched sufficiently to significantly lower the cross section. This has also been observed for metal carbonyls on Ag(111).[5,9]

4.2. Photochemistry at 532 nm. Improbable processes at surfaces can often be due to the fact that they can only occur at some special defects at the surface, such as steps or kinks, which are always present but with small probability. Very small cross sections for photodissociation and desorption could have the same origin, see e.g. ref 42. The cross section at 532 nm is a factor of 100 smaller than at 266 nm. Nevertheless, we feel that the TOF spectrum observed at 532 nm for a coverage of one monolayer is not due to a minority of the adsorbed molecules but is most likely due to the entire adsorbed layer. This is apparent from a comparison of the TOF yields at 532 and 266 nm. The cross section measurements show that after 6800 shots of 24 and 3.9 mJ cm^{-2} for 532 and 266 nm, respectively, the majority of the photoactive molecules have dissociated. Hence, no specific sites seem required. For a coverage of 1 ML at 266 nm we concluded above that one complete monolayer could be dissociated. Comparing the yields at 1 ML for both wavelengths and realizing that in both cases the majority of the photoactive molecules have dissociated, it is concluded that at 532 nm for a coverage of 1 ML a complete layer can also be converted.

The observed TOF traces at 532 nm are not caused by substrate heating by the laser for the following reasons. At heating rates of 1 Ks^{-1} in TDS no thermal dissociation is observed, only desorption is present. At the much higher heating rates induced by the picosecond laser, desorption is generally favored over dissociation.[43] Since no laser-induced thermal desorption is observed, the dissociation is unlikely to have a thermal origin. Besides this qualitative approach a quantitative argument can also be made. At the lowest intensity used only 0.5 mJ cm^{-2} of energy is absorbed by the substrate. Calculations show that the temperature rise induced by these pulses is limited to a few hundreds of degrees, which is insufficient to desorb the *tert*-butyl nitrite molecule during this picosecond pulse.[44,45] Thermal dissociation is even more improbable because the fast heating induced by the picosecond laser favors desorption. If laser heating were important, highly nonlinear dependencies of the desorption yield on the laser power are to be expected. Those have not been observed.

From the linearity in the yield with intensity (not shown) we can conclude that dissociation at 532 nm is caused by a single photon excitation. The qualitatively different results for 532 and 266 nm excluded the possibility that at 532 nm dissociation is caused by minute amounts of fourth harmonic in the beam. The spacer layer experiments exclude a substrate-mediated mechanism. So, the conclusion must be that at 532 nm *tert*-butyl nitrite dissociation is caused by a direct excitation mechanism. This is in contrast to what is commonly assumed in the gas phase papers where generally dissociation in the visible is believed to be absent. A direct excitation mechanism at 532 nm is conceivable. Gas phase studies never investigated the upper limit of a possible dissociation cross section in the visible. If an estimation is made of this upper limit from available absorption spectra,[23,46] a value low into the 10^{-21} decade is obtained. The value of 3×10^{-21} cm^2 found in this study is consistent with such an upper limit. For HONO, a

molecule with the same functional group and a very similar absorption structure in the 300−400 nm regime, dissociation into NO and HO was found down to 585 nm.[47,48] This finding also indicates that a direct channel at 532 nm is conceivable. Dissociation at 532 nm is also possible from an energetic point of view, the 2.3 eV photons exceed the dissociation energy of 1.8 eV. The remaining 0.5 eV is more than sufficient to provide 0.15 eV translational energy to the NO photoproduct.

The spacer layer experiment and the yield measurement (Figures 3 and 5) show that for high coverages, dissociation mainly occurs in the top layer of the film. Deeper layers are incapable in producing NO. That hyperthermal NO is still observed at high coverages also shows that only in the outermost layer dissociation is possible. Caging is very likely the cause of the absence of dissociation in the inner multilayers.

In the monolayer regime the ratio between hyperthermal and thermal NO at 532 nm is very similar to the ratio at 355 nm (see for example the TOF spectra). This indicates that at both wavelengths thermalization by the substrate occurs. The translational energy of the thermal component in the submonolayer regime is not completely thermal as is apparent by the elevated values compared to the substrate temperature (Figure 2). With completion of the monolayer the degree of thermalization increases. This suggests that scattering of NO molecules with adsorbates also increases the degree of thermalization. Comparison with the results obtained at MgF_2 shows that the Ag(111) substrate is instrumental in separating the two contributions. For higher coverages things appear to be different. At 532 nm the spacer layer experiments suggest that NO is also thermalized in the top of the *tert*-butyl nitrite film. Also the ratio between hyperthermal and thermal NO changes drastically with coverage. This all points toward another thermalization mechanism in the film, the nature of which is not clear.

5. Conclusions

Dissociation of *tert*-butyl nitrite at 266 nm results in higher translational energies, compared to dissociation at 355 nm. The cross section at 266 nm is an order of magnitude higher than at 355 nm, and a direct excitation mechanism is responsible for dissociation. This is consistent with an excitation into the dissociative S_2 state at 266 nm. But although dissociation at 355 and 266 nm may proceed via different states, the characteristics are very similar. In both cases NO is the only desorbing product, and part of the NO is trapped and thermalized by the substrate. Caging prevents dissociation in the multilayer for both wavelengths.

At 532 nm dissociation via a direct excitation is observed with a cross section of 3×10^{-21} cm^2. Because of this conclusion, the presence of dissociation in the gas phase at this wavelength should be reinvestigated. At 532 nm on Ag(111) also a hyperthermal and a thermal NO desorption distribution are measured.

Acknowledgment. The authors would like to thank F. G. Giskes and R. Schaafsma for technical support. W. J. van der Zande and M. A. Gleeson are thanked for their constructive comments on the manuscript. L.P. thanks the European Union for an institutional fellowship (ERBCHB6CT 940701). This work is part of the research program of the "Stichting voor Fundamenteel Onderzoek der Materie (FOM)", which is financially supported by the "Nederlandse organisatie voor Wetenschappelijk Onderzoek (NWO)".

References and Notes

(1) Jenniskens, H. G.; van Essenberg, M.; Kadodwala, M.; Kleyn, A. W. *Chem. Phys. Lett.* **1997**, *268*. 7.
(2) Jenniskens, H. G.; Philippe, L.; van Essenberg, W.; Kadodwala, M.; Kleyn, A. W. *J. Chem. Phys.* **1998**, *108*, 1688.
(3) Marsh, E. P.; Schneider, M. R.; Gilton, T. L.; Tabares, F. L.; Meier, W.; Cowin, J. P. *Phys. Rev. Lett.* **1988**, *60*, 2551.
(4) Marsh, E. P.; Gilton, T. L; Meier, W.; Schneider, M. R.; Cowin, J. P. *Phys. Rev. Lett.* **1988**, *61*, 2725.
(5) So, S. K.; Ho, W. *J. Chem. Phys.* **1991**, *95*, 656.
(6) Weik, F.; de Meijere, A.; Hasselbrink, E. *J. Chem. Phys.* **1993**, *99*, 682
(7) Zhu, X.-Y. *Annu. Rev. Phys. Chem.* **1994**, *45*, 113.
(8) Ho, W. *Surf. Sci.* **1996**, *363*, 166.
(9) Henderson, M.; Ramsier, R.; Yates, J. *Surf. Sci.* **1992**, *275*, 297.
(10) Pressley, L. A.; Pylant, E. D.; White, J. M. *Surf. Sci.* **1996**, *367*. 1.
(11) Pylant, E.; Junker, K.; Szulczewski, G.; Hubbard, M.; White, J. *J. Phys. Chem. B* **1997**, *101*, 4803.
(12) Szulczewski, G.; White, J. *J. Vac. Sci. Techn. A* **1997**, *15*, 1526.
(13) Junker, K.; White, J. *Surf. Sci.* **1997**, *382*, 67.
(14) Schwartz-Lavi, D.; Bar, I.; Rosenwaks, S. *Surf. Sci.* **1978**, *76*, 531.
(15) Inoue, G.; Kawasaki, M.; Sato, H.; Kikuchi, T.; Kobayashi, S.; Arikawa, T. *J. Chem. Phys.* **1987**, *87*, 5722.
(16) Keller, B. A.; Felder, P.; Huber, J. R. *J. Phys. Chem.* **1987**, *91*, 1114.
(17) Lavi, R.; Schwartz-Lavi, D.; Bar, I.; Rosenwaks, S. *J. Phys. Chem.* **1987**, *91*, 5398.
(18) August, J.; Brouard, M.; Docker, M. P.; Milne, C. J.; Simons, J. P.; Lavi, R.; Rosenwaks, S.; Schwartz-Lavi, D. *J. Phys. Chem.* **1988**, *92*, 5485.
(19) Schwartz-Lavi, D.; Rosenwaks, S. *J. Chem Phys.* **1988**, *88*, 6922.
(20) Winniczek, J. W.; Dubs, R. L.; Appling, J. R. McKoy, V.; White, M. G. *J. Chem. Phys.* **1989**, *90*, 949.
(21) Effenhauser, C. S.; Felder, P.; Huber, J. R. *J. Phys. Chem.* **1990**, *94*, 296.
(22) Sutter, H. U.; Brühlmann, U.; Huber, J. R. *Chem. Phys. Lett.* **1990**, *171*, 63.
(23) Hippler, M.; McCoustra, M. R. S.; Pfab, J. *Chem. Phys. Lett.* **1992**, *198*, 168.
(24) Hippler, M.; Al-Janabi, F. A. H.; Pfab, J. *Chem. Phys. Lett.* **1992**, *192*, 173.
(25) Kades, E.; Rösslein, M.; Huber, J. R. *Chem. Phys. Lett.* **1993**, *209*, 275.
(26) Mestdagh, J. M.; Berdah, M.; Dimicoli, I.; Mons, M.; Meynadier, P.; d'Oliveira, P.; Piuzzi, F.; Visticot, J. P.; Jouvet, C.; Lardeux-Dedonder, C.; Martrenchard-Barra, S.; Soep, B.; Solgadi, D. *J. Chem. Phys.* **1995**, *103*, 1013.
(27) Rösslein, M.; Kades, E.; Bergmann, K.; Huber, J. R. *Chem. Phys. Lett.* **1995**, *235*, 242.
(28) Kades, E.; Rösslein, M.; Brühlmann, U.; Huber, J. R. *J. Phys. Chem.* **1993**, *97*, 989.
(29) Kades, E.; Rösslein, M.; Huber, J. R. *J. Phys. Chem.* **1994**, *98*, 13556.
(30) Bergmann, K.; Huber, J. R. *J. Phys. Chem. A* **1997**, *101*, 259.
(31) Calvert, J. G.; Pitts, J. M. *Photochemistry*; Wiley: New York, 1966.
(32) Schwartz-Lavi, D.; Bar, I.; Rosenwaks, S. *Chem. Phys. Lett.* **1984**, *109*, 296.
(33) Jenniskens, H. G.; van Essenberg, W.; Kadodwala, M.; Kleyn, A. W. *Surf. Sci.* **1998**, *402*−*404*, 140.
(34) Simpson, C. J. S. M.; Griffiths, P. T.; Towrie, M. *Chem. Phys. Lett.* **1995**, *234*, 203.
(35) Simpson, C. J. S. M.; Griffiths, P. T.; Wallaart, H. L.; Towrie, M. *Chem. Phys. Lett.* **1996**, *263*, 19.
(36) Jenniskens, H. G.; Bot, A.; Dorlandt, P. W. F.; van Essenberg, W.; de Haas, E.; Kleyn, A. W. *Meas. Sci. Technol.* **1997**, *8*, 1313.
(37) Jenniskens, H. G.; Dorlandt, P. W. F.; Kadodwala, M. F.; Kleyn, A. W. *Surf. Sci.* **1996**, *357*−*358*, 624.
(38) Zhou, X. L. Zhu, X. Y.; White, J. M. *Surf. Sci. Report* **1991**, *13*, 73.
(39) Sack, N. J.; Akbulut, M.; Madey, T. E. *Phys. Rev. Lett.* **1994**, *73*, 794.
(40) Akbulut, M.; Sack, N. J.; Madey, T. E. *Phys. Rev. Lett.* **1995**, *75*, 3414.
(41) Akbulut, M.; Sack, N. J.; Madey, T. E. *Surf. Sci. Report* **1997**, *28*, 177.
(42) Shea, M.; Compton, R. *Phys. Rev. B* **1993**, *47*, 9967.
(43) Hall, R. B. *J. Phys. Chem.* **1988**, *91*, 1007.
(44) Bechtel, J. H. *J. Appl. Phys.* **1975**, *46*, 1585.
(45) Burgess, D., Jr.; Stair, P. C.; Weitz, E. *J. Vac. Sci. Techn. A* **1986**, *4*, 1362.
(46) Fitzmaurice, D. J.; Frei, H. *Chem. Phys. Lett.* **1992**, *192*, 166.
(47) Cox, R. A. *J. Photochem.* **1974**, *3*, 175.
(48) Cox, R. A. *J. Photochem.* **1974**, *3*, 291.